

## Critical fluctuations in a soliton formation of attractive Bose-Einstein condensates

Rina Kanamoto,<sup>1</sup> Hirotaki Saito,<sup>2</sup> and Masahito Ueda<sup>2,3</sup><sup>1</sup>Department of Physics, Osaka City University, Osaka 558-8585, Japan<sup>2</sup>Department of Physics, Tokyo Institute of Technology, Tokyo 152-8551, Japan<sup>3</sup>ERATO, Japan Science and Technology Corporation (JST), Saitama 332-0012, Japan

(Dated: February 23, 2019)

We employ mean-field, Bogoliubov and many-body theories to study critical fluctuations in the position and momentum of a Bose-Einstein condensate whose translation symmetry is spontaneously broken due to attractive interactions. In a homogeneous system, the many-body ground state of the symmetry-preserving Hamiltonian is very fragile against superposition of low-lying states, while the mean-field theory predicts a stable bright soliton which spontaneously breaks translation symmetry. We show that weak symmetry-breaking perturbations cause the translation-symmetric many-body ground state to cross over to a many-body bright soliton. We argue that the center-of-mass fluctuations in the soliton state arise primarily from the depletion of the condensate to translation modes. We develop an extended mean-field theory to analytically reproduce these results obtained by the exact diagonalization method.

PACS numbers: 03.75.Lm, 03.75.Nt, 03.65.Ta

## I. INTRODUCTION

Ultracold matter waves offer the possibility of observing quantum-mechanical fluctuations associated with low-dimensional many-body effects and phase transitions [1, 2, 3, 4, 5]. In Bose-Einstein condensates (BECs) of dilute gases, various techniques of controlling experimental parameters enable us to study a rich variety of phase transitions. A standard way to study a ground-state phase of the condensate is to introduce an order parameter with spontaneously broken symmetry. On the other hand, quantum fluctuations play a crucial role in the emergence of the order parameter, and the related issues have been widely studied in the systems of BECs [6, 7, 8, 9, 10, 11, 12, 13]. Furthermore, since atomic condensates are on the mesoscopic scale, we may expect interesting finite-size effects which are absent in the thermodynamic limit.

The exact many-body ground state of a one-dimensional (1D) system with translation symmetry does not exhibit the off-diagonal long-range order in the thermodynamic limit. The ground state has the translation symmetry of the original Hamiltonian, but is extremely fragile against localization to a bright soliton when the interaction is attractive. By investigating the many-body energy spectrum of this system, we have found that there exists a large number of low-lying quasidegenerate many-body eigenstates, and the localization to a soliton is due to the superposition of these states [14]. In the thermodynamic limit, the energy gap between the ground and low-lying states vanishes, and therefore the localization occurs no matter how small the symmetry-breaking perturbation is. Such a localized soliton [15] can be well described by the Gross-Pitaevskii (GP) equation. However, in a mesoscopic system, an energy gap between the ground and low-lying excited states remains finite, and therefore we can expect a crossover between the state with the translation symmetry and the soliton state

as a function of the strength of interaction. In such a crossover regime, quantum fluctuations are expected to be large and the localization process is nontrivial.

The aim of this paper is to examine the critical fluctuations in a soliton formation of an attractive BEC. We consider two cases for the breaking of translation symmetry, that is, symmetry-breaking potentials and quantum measurements. We tackle this problem using the numerical diagonalization of the Hamiltonian and an extended mean-field theory. In particular, we explicitly calculate the uncertainty relation between the center-of-mass position and momentum, and show that the inclusion of center-of-mass fluctuations of the soliton is crucial for understanding the nature of the many-body ground state. These fluctuations emerge as a depletion of the condensate, and decrease with increasing the magnitude of the symmetry-breaking potential or the number of the measurements.

This paper is organized as follows. In Sec. II, we introduce a model of a 1D attractive BEC system with the periodic boundary condition, and briefly review the many-body energy spectrum and ground-state properties of the uniform system. In Sec. III, we introduce a symmetry-breaking perturbation, a symmetric-breaking potential, a double-well potential, and quantum measurements, and discuss critical fluctuations in the position and momentum of symmetry-broken states. In Sec. IV, we construct the Bogoliubov ground state that incorporates the effect of center-of-mass fluctuations due to the presence of the finite-size potential. We also propose an extended mean-field theory to describe the effect of quantum measurements on the uncertain relation between the position and the momentum. In Sec. V, we summarize the main results of this paper.

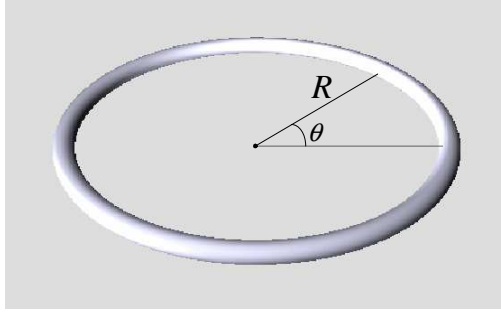


FIG. 1: (Color online) Schematic illustration of a quasi-one-dimensional torus.

### III. QUANTUM PHASE TRANSITION IN AN ATTRACTIVE BEC

#### A. Many-body eigenstates

We consider a system of weakly interacting bosons on a quasi-1D torus with radius  $R$  as schematically illustrated in Fig. 1. Throughout this paper the length, angular momentum, and energy are measured in units of  $R$ ,  $\sim$ , and  $\sim^2 = (2/R)$ , respectively. The Hamiltonian of the system is given by

$$\hat{H} = \int_0^{2\pi} d\theta \left( \hat{y}^2(\theta) \frac{\partial^2}{\partial \theta^2} \hat{y}(\theta) - \frac{g}{2} \hat{y}^2(\theta) \hat{y}^2(\theta) \right); \quad (1)$$

where  $\theta$  is the azimuthal angle,  $\hat{y}$  is the boson field operator obeying the periodic boundary condition  $\hat{y}(\theta) = \hat{y}(\theta + 2\pi)$ , and the interaction is assumed to be attractive ( $g > 0$ ). Although the Hamiltonian (1) is exactly solvable and the exact solution is analytically obtained by the Bethe ansatz [16], in principle, the solution is intractable for a large number of atoms. On the other hand, the configuration interaction method can evaluate the ground-state energy rather accurately [17]. Experimentally the quasi-1D ring-shaped BEC has recently been realized in a circular magnetic trap [18].

We employ a numerical diagonalization method to investigate many-body eigenstates of the Hamiltonian (1) by restricting the Hilbert space to that spanned by the angular momentum  $l=0, 1$  states. It is possible to extend the calculation to including the  $l=2, 3$  states. However, all results obtained for  $l=0, 1$  remain qualitatively unchanged, and we thus restrict ourselves to  $l=0, 1$  unless otherwise stated (see Sec. III B). The Fock-state bases are thus written as  $|j_1; n_0; n_1\rangle$ , where  $n_1$  is the number of atoms with angular momentum  $l$ . The number of atoms and the total angular momentum are given by  $n_1 = N$ , and  $l = L$ , respectively. The field operator is thus expanded as

$$\hat{y}(\theta) = \frac{1}{2} (\hat{c}_0 + \hat{c}_1 e^{i\theta} + \hat{c}_1 e^{-i\theta}); \quad (2)$$

where  $\hat{c}_l$  is the annihilation operator of a boson with angular momentum  $l$ .

Figure 2 shows the low-lying many-body spectrum of the Hamiltonian  $\hat{H}$ , in which extensive rearrangement of the distribution of the eigenstates is seen to occur at  $gN \approx 1$  due to the quantum phase transition. We see that in  $gN \approx 1$  the spectrum is classified by two indices: that is, the band index  $\lambda$  and the angular momentum index  $L$  characterize each level as

$$\hat{H} |j_L\rangle = E_{\lambda, L} |j_L\rangle; \quad (3)$$

where

$$|j_L\rangle = \prod_n A_n |j_n; n; N - 2n - L; n + L\rangle; \quad (4)$$

The energy levels  $E_{\lambda, L}$  in band  $\lambda$  are distributed according to  $E_{\lambda, 0} < E_{\lambda, 1} < E_{\lambda, 2} < \dots$ . For  $0 < gN < 1$ , on the other hand, some  $E_{\lambda, L}$ 's are almost degenerate. To understand the nature of the rearrangement at  $gN \approx 1$ , we first study the eigenstates in the absence of interaction  $gN = 0$ , where the eigenstates can be described by Fock states  $|j_1; n_0; n_1\rangle$ . We define the  $J$ th state ( $J = 0; 1; 2; \dots$ ) as the one in which  $J$  atoms are excited. For example, the  $J = 0$  state corresponds to the noninteracting ground state given by

$$|J = 0\rangle = |0; 0; \dots; 0\rangle; \quad (5)$$

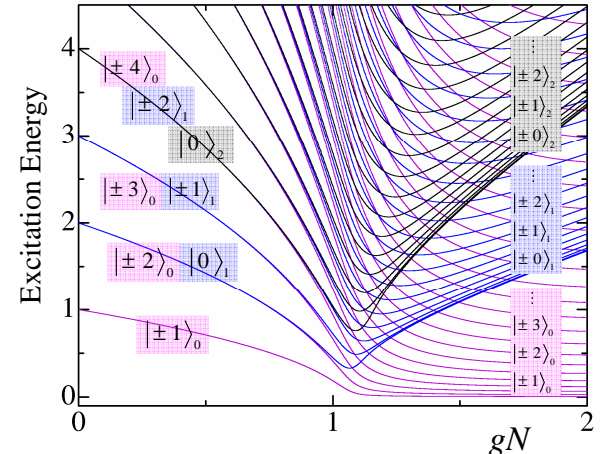


FIG. 2: (Color online) Many-body excitation spectrum  $E_{\lambda, L}$  vs  $gN$  of the Hamiltonian  $\hat{H}$  with  $N = 200$ , where  $L$  is the angular momentum index and  $\lambda$  is the index of the bands that appears for  $gN \approx 1$ . We plot only low-lying states with indices  $\lambda = 0, 1$ , and  $2$ . The state  $|j_L\rangle$  denotes the many-body eigenstate whose total angular momentum is  $L$  and band index is  $\lambda$ .

and the excited states are given as

$$\begin{aligned}
 J = 1 &: j \quad 1i_0 = j;N \quad 1;0i; \\
 J = 1 &: jli_0 = j;N \quad 1;li; \\
 J = 2 &: j \quad 2i_0 = j;N \quad 2;0i; \\
 J = 2 &: jli_1 = j;N \quad 2;li; \\
 J = 2 &: j2i_0 = j;N \quad 2;2i; \\
 J = 3 &: j \quad 3i_0 = j;N \quad 3;0i; \\
 &\vdots
 \end{aligned} \tag{6}$$

The  $J$ th state is hence  $(J+1)$ -fold degenerate. The index  $l$ , which is the band index in  $gN$  & 1, corresponds to the number of  $l = 1$  pairs in the Fock state for each  $J$ th state at  $gN = 0$ , ie.,  $(J - l)_{j=2} = 0; 1; 2; \dots$ . For  $0 < gN \leq 1$ , the levels are characterized by  $J$  alone, since the degeneracy with respect to  $l$  at  $gN = 0$  is maintained.

The excitations in  $0 < gN < 1$  have substantial energy gaps until the critical point  $gN = 1$  is reached. On the other hand, for  $gN > 1$ , the energy difference between the ground and the first excited states scales as  $1/N$ . We thus expect that the ground state for  $gN > 1$  is vulnerable for large  $N$ , and perturbations of the order  $1/N$  can cause drastic reconstruction of the ground state. The emergence of these quasidegeneracies in the energy spectrum may be regarded as a precursor of symmetry breaking, and interesting effects such as the enhancement of the condensate fraction [14] can be expected as a consequence of symmetry breaking.

for a many-body state  $j$  are given in terms of the maximum eigenvalue  $\lambda_M$  and the corresponding eigenfunction of the reduced single-particle density matrix

( $^0$ ;  $\hat{h}$ ) =  $\hat{h} \hat{j}^y ({}^0) \hat{j} (j)$   $j \in \mathbb{N}$ . If the maximum eigenvalue  $m$  is on the order of unity and the other ones are on the order of  $1/N$ , there exists a usual single condensate described by the corresponding eigenfunction. For the case of  $gN \approx 1$ , however, the ground state does not fall into this category of BEC. By calculating the eigenvalue of  $\hat{h}$  for the ground state as a function of  $gN$ , we find that  $m$  is on the order of 1 for  $gN \approx 1$ , but for  $gN \approx 1$  there appears more than one eigenvalue on the order of unity. The ground state is thus a conventional single condensate for  $gN \approx 1$ , and fragmented [20] for  $gN \approx 1$ .

Since we consider the Hamiltonian with translation symmetry, the expectation value of the number density of particles  $n(\vec{r}) = N(\vec{r}; \vec{r})$  of the ground-state wave function is constant for  $0 \leq \vec{r} \leq 2\pi$ . In contrast, the two-body correlation function,

$$g^{(2)}( ; ^0) = \frac{h^{\gamma_y}( )^{\gamma_y}( ^0)^{\gamma}( ^0)^{\gamma}( )i}{h^{\gamma_y}( )^{\gamma}( )ih^{\gamma_y}( ^0)^{\gamma}( ^0)i}; \quad (7)$$

is found to deviate greatly from unity for  $gN \gg 1$ , while it is almost unity for  $gN \ll 1$  [21]. We show in Fig. 3 the Fano factor of the ground state defined by

$$F(\ ) = \frac{h n^2(\ ) i - h n(\ ) i^2}{n(\ ) h^2} = 1 + n(\ ) g^{(2)}(\ ; \ ) \quad 1: \quad (8)$$

The large deviation of  $F(\cdot)$  from unity for  $gN \gg 1$  indicates that the number density of particles has quantum fluctuations, which may also be regarded as a precursor of formation of the broken-symmetry state.

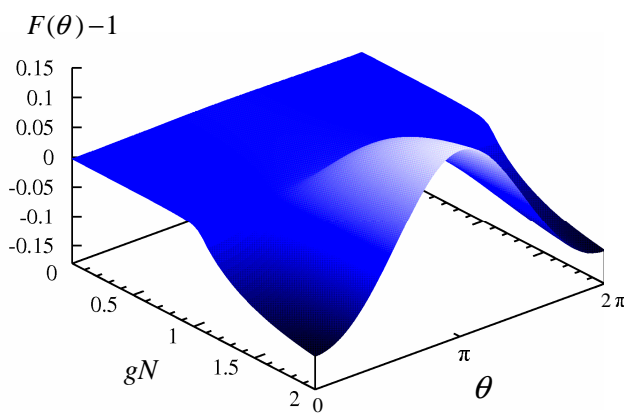


FIG. 3: (Color online) Fano factor  $F(\theta)$  in Eq. (8) of the many-body ground-state wave function as functions of the strength of the interaction  $g_N$  and azimuthal angle  $\theta$  with  $N = 200$ .

### III. SYMMETRY-BREAKING PERTURBATIONS

In this section, we investigate on how the many-body ground state responds to infinitesimal symmetry-breaking potentials or quantum measurements.

### A. infinitesimal potential

## 1. Superposition of low-lying states

We employ the exact diagonalization method to obtain the ground state of the Hamiltonian

$$\hat{K}_1 = \hat{H} + "1 \hat{V}_1; \quad (9)$$

where  $\hat{V}_1 = \begin{smallmatrix} R_2 & 0 \\ 0 & 0 \end{smallmatrix} d^\gamma(\cdot) \cos^\gamma(\cdot)$  is a symmetry-breaking potential. Since we discuss here only low-lying modes ( $\ell = 0; L \neq 0$ ) close to the ground state

( $\ell = 0; L = 0$ ), we simplify the notations of the eigenstates by omitting the index  $\ell$ .

We consider the energy change in the many-body ground state as a function of the magnitude  $\kappa_1$  of the potential. Because of the degeneracy  $E_L = E_{-L}$  with respect to the angular momentum, we assume that the broken-symmetry ground state  $j^{(\kappa_1)}_i$  of the Hamiltonian  $\hat{K}_1$  is described by

$$j^{(\kappa_1)}_i = e^{i\hat{p}_i} j^{(0)}_i + \frac{X}{L} (j_{-i} + j_{-L}) \quad (10)$$

where the coefficients  $j_L$  satisfy the normalization condition,  $\sum_L j_L \neq 0$ .

In Fig. 4, we show the energy change in the ground states

$$E_{\text{gs}} = h^{(\kappa_1)} \hat{K}_1 j^{(\kappa_1)}_i - h^{(0)} \hat{p}_i \quad (< 0); \quad (11)$$

multiplied by  $N$ , as a function of

$$\kappa_1 N^2: \quad (12)$$

The slope of the  $\kappa_1$  dependence of  $E_{\text{gs}}$  changes near  $\kappa_1 = 1$ . The  $\kappa_1$  dependence of  $E_{\text{gs}}$  for  $0 < \kappa_1 < 1$  can be estimated by perturbation theory. The first-order correction to the ground-state energy is zero, and the second-order correction is given by

$$E^{(2)} = \frac{X}{L \neq 0} \frac{j_L j_1 \hat{V}_1 \hat{p}_i}{E_0 - E_L}; \quad (13)$$

where the denominator and the numerator are on the order of  $N^{-1}$  and  $(\kappa_1 N)^2$ , respectively. The energy difference  $E_{\text{gs}}$  therefore depends on  $\kappa_1 N^3 = \kappa_1^2 N$ . At the transition point  $\kappa_1 = 1$ , the shift in the ground-state energy due to the symmetry-breaking perturbation is  $E_{\text{gs}} j' \neq N$ , which is on the same order of magnitude as the energy gap. As  $\kappa_1$  exceeds unity, the energy scale of the potential exceeds the energy gap  $E_1 - E_0$  and the matter wave begins to localize by superposing the ground and low-lying excited states as shown in Fig. 5(a). The perturbation theory, therefore breaks down for  $\kappa_1 > 1$ . The  $\kappa_1$  dependence in this regime can be well described by the mean-field theory as shown in Sec. IV B 1. In the absence of the symmetry-breaking potential, the formation of the broken-symmetry state  $j^{(\kappa_1)}_i$  costs energy by an amount of

$$E_{\text{sup}} = h^{(\kappa_1)} \hat{K}_1 j^{(\kappa_1)}_i - h^{(0)} \hat{p}_i$$

$$= (E_L - E_0) j_L \neq 0; \quad (14)$$

which gives an energy increase associated with the superposition of the low-lying state.

The symmetry breaking must be associated with a Nambu-Goldstone mode, which plays the role of restoring the symmetry. In the present context, the Nambu-Goldstone mode should be the translation zero mode

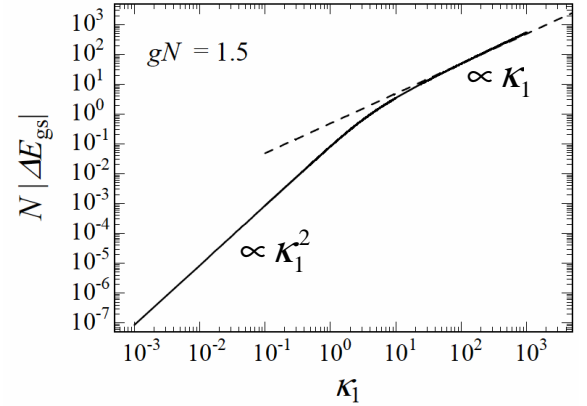


FIG. 4: The amount of decrease in the ground-state energy given by Eq. (11) in the presence of a symmetry-breaking potential for  $gN = 1.5$ , where  $\kappa_1 = \kappa_1 N^2$ . The superimposed dashed line shows the result of the mean-field calculation given in Eq. (37).

$j^{(\kappa_1)}_i$  of the localized state  $j^{(\kappa_1)}_i$  which is defined as

$$j^{(\kappa_1)}_i = \frac{d}{d\kappa_1} j^{(\kappa_1)}_i$$

$$= ie^{i\hat{p}_i} \frac{X}{L} (j_{-i} + j_{-L}); \quad (15)$$

The broken-symmetry state with the excitation to the translation mode is thus given by

$$j^{(\kappa_1)}_i = p \frac{1}{1 + j^{(\kappa_1)}_i} j^{(0)}_i + \frac{1}{N_{\text{tr}}} j^{(\kappa_1)}_i; \quad (16)$$

where  $p$  denotes the relative amplitude of the excitation, and the energy difference associated with the excitation of the translation mode is given by

$$E_{\text{tr}} = h^{(\kappa_1)} \hat{K}_1 j^{(\kappa_1)}_i - h^{(0)} \hat{p}_i$$

$$= \frac{j^{(\kappa_1)}_i}{1 + j^{(\kappa_1)}_i} h^{(\kappa_1)} \hat{K}_1 j^{(\kappa_1)}_i$$

$$+ \frac{1}{N_{\text{tr}}} h^{(\kappa_1)} \hat{K}_1 j^{(\kappa_1)}_i; \quad (17)$$

where  $N_{\text{tr}} = h^{(\kappa_1)} j^{(\kappa_1)}_i$ . We note that  $E_{\text{tr}}$  becomes zero in the limit of  $\kappa_1 \rightarrow 0$ .

## 2. Quantum fluctuations in position and momentum

Let us investigate the quantum fluctuations in the ground state  $j^{(\kappa_1)}_i$  as a function of the magnitude of the symmetry-breaking potential. The angular-momentum distribution is given by  $j_L \neq = j_L j^{(\kappa_1)}_i \neq$ , which becomes Gaussian-like for  $\kappa_1 \ll 1$  as shown in Fig. 6(a). In Fig. 6(b) we plot the variance  $(L)^2$  of the angular-momentum distribution with open circles. The deviation in  $\kappa_1$  dependence of  $(L)^2$  in  $0 < \kappa_1 < 1$  arises

because in this region the energy scale of the symmetry-breaking potential is smaller than the energy gap between the ground and the first excited states, and the angular momentum fluctuation is suppressed. Once the matter wave is localized by the superposition of the form (10), the fluctuation  $L$  of the angular momentum distribution is proportional to  $\kappa_1^{1/4}$ .

It follows from the uncertainty relation  $L \approx \kappa_1$  that the center-of-mass fluctuation of the localized state  $j^{(\kappa_1)}(r)$  for  $\kappa_1 \ll 1$  is given by

$$\text{cm} : \langle L \rangle \approx \kappa_1^{1/4}; \quad (18)$$

which is significant for small perturbations [22]. In Sec. IV B, we will show that this  $\kappa_1$  dependence is well described by the Bogoliubov ground state that takes into account this position fluctuation by the depletion of the condensate.

### 3. Condensate fraction

By using the many-body ground state  $j^{(\kappa_1)}(r)$  in the presence of the symmetry-breaking potential, and diagonalizing the single-particle density matrix  $(L; \vec{r}) = h^{(\kappa_1)} \vec{f}_{\vec{r}}^{\dagger} \vec{f}_{\vec{r}}$ , we obtain the three eigenvalues in the

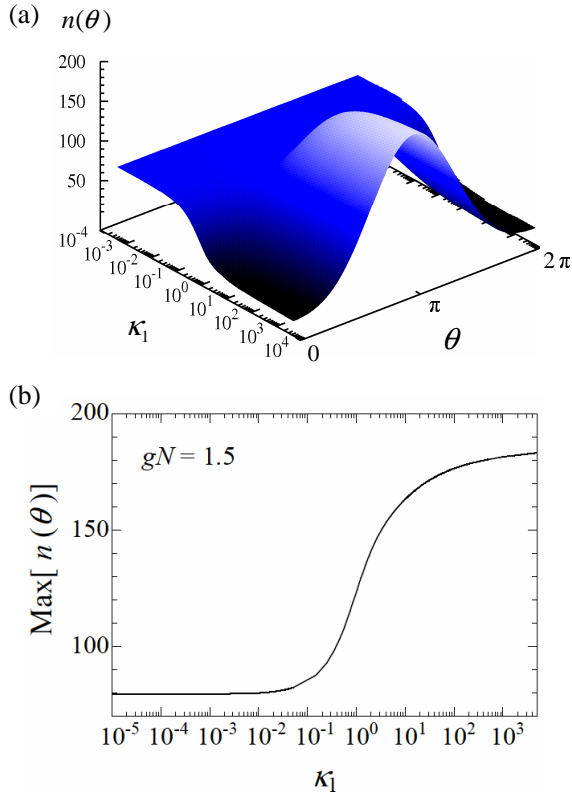


FIG. 5: (Color online) (a) Density profile  $n(\theta)$  of the many-body wave function and (b) the peak density as a function of  $\kappa_1$ .

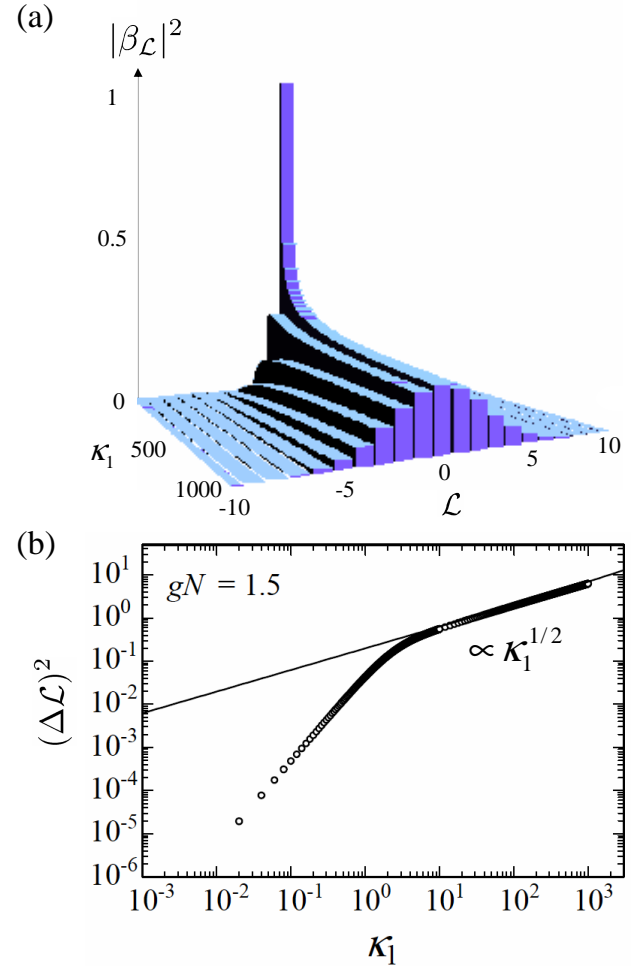


FIG. 6: (Color online) (a) Distribution  $|\beta_L|^2$  of the angular momentum  $L$  in the many-body ground state  $j^{(\kappa_1)}(r)$  for  $gN = 1.5$ . (b) Width of angular momentum distribution in the many-body ground state  $j^{(\kappa_1)}(r)$  (open circles) and that in the Bogoliubov ground state  $j^{(B)}(r)$  (solid line) given by Eq. (55).

truncated bases. We define the number of depleted atoms  $N^0$  of the many-body ground state as  $N^0 = N - 1 - j^{(\kappa_1)}$ , where  $j^{(\kappa_1)}$  is the maximum eigenvalue of  $\hat{n}$ . We plot  $N^0/N$  in Fig. 7 as a function of  $\kappa_1$ . For  $\kappa_1 = 0$ , the maximum depletion is obtained due to the fragmentation of the many-body ground state, and it remains constant for  $\kappa_1 < 1$ . The depletion  $N^0$  suddenly begins to decrease at  $\kappa_1 = 1$ , and the  $\kappa_1$  dependence for  $\kappa_1 > 1$  is found to be  $\kappa_1^{-1/2}$ . The condensate fraction thus increases when the ground state begins to localize.

### B. Case of a double-well potential

We next discuss what happens when there exists a symmetric double-well potential of the form  $V_2(r) = \cos^2 r$ ,

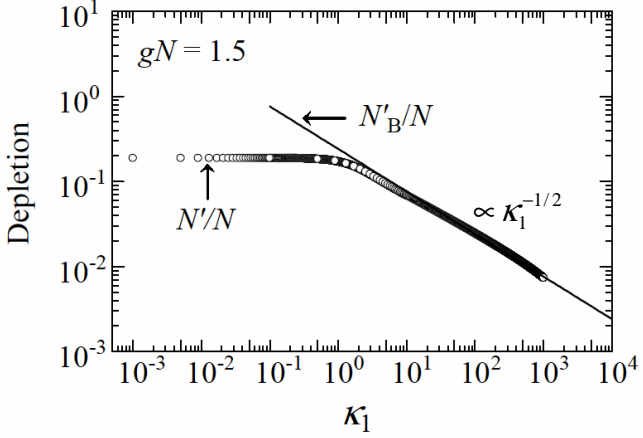


FIG. 7: Depletions of the condensate obtained by the diagonalization of the Ham iltonian (open circles) and by the

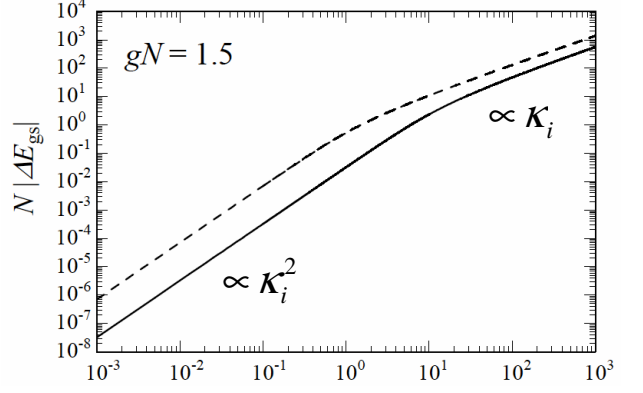


FIG. 9: G round-state energy as a function of  $K_2$  (solid curve) in the presence of a double-well potential measured from  $E_0 = \hbar \hat{J}_1 \hat{J}_2$ . Dashed curve shows the results of a single-well potential.

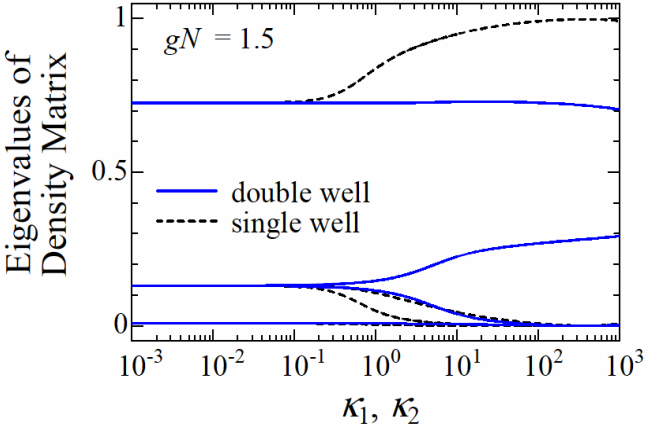


FIG. 8: (Color online) Eigenvalues of the reduced single-particle density matrix for the double-well potential (solid curves) as a function of  $K_2 = K_1 N^2$ . Dashed curves show the results obtained for a single-well potential as a function of  $K_1 = K_1 N^2$ . In the latter case only one large eigenvalue survives for  $K_1 \gg 1$ .

and discuss the ground state of the Ham iltonian

$$\hat{K}_2 = \hat{H} + K_2 \hat{V}_2; \quad (19)$$

where

$$\hat{V}_2 = \int_0^{Z_2} d\mathbf{r} \hat{\psi}^\dagger(\mathbf{r}) V_2(\mathbf{r}) \hat{\psi}(\mathbf{r}); \quad (20)$$

In the double-well potential, a rich variety of experiments, e.g., diagnosing the correlation functions from interference and uncertainty relations, become possible [3, 23].

For an attractive condensate in a sufficiently deep symmetric double-well potential, the ground state may form a Schrodinger's cat state, where the localized macroscopic states on the left and the right wells are in a superposition

state [24, 25, 26, 27]. We diagonalize the Ham iltonian  $\hat{K}_2$  including angular momentum states  $l=0, 1, 2$  because the symmetry of the potential requires the inclusion of the  $l=2$  states. The solid curves in Fig. 8 show eigenvalues of the reduced single-particle density matrix. The presence of more than one large eigenvalue is a signature of the Schrodinger's cat state. While the maximum eigenvalue  $\lambda_1$  increases with increasing  $K_2$ , it decreases slowly with increasing  $K_1$ , and simultaneously the second maximum eigenvalue  $\lambda_2$  begins to grow. These eigenvalues  $\lambda_{1,2}$  eventually approach 1=2, corresponding to the states localized on the one or the other well.

In the case of the double-well potential, the many-body ground state is also described by the superposition in the form of Eq. (10). Figure 9 shows that the  $K_2$  dependence of the energy difference  $\hbar \hat{J}_2 \hat{J}_1 = \hbar \hat{J}_1 \hat{J}_2$  is similar to that of the single-potential case shown as a dashed curve. This indicates that the superposition begins near  $K_2 \approx 1$ , since the energy at that point is of the order  $1=N$ .

### C. Quantum measurement

We next consider quantum fluctuations caused by repeated measurements. The issue of interference of the two independent BECs was discussed from the viewpoint of quantum measurements in Refs. [28, 29]. Below we discuss an analogous process in which a fragmented condensate makes a transition to a single condensate via a quantum measurement [14, 30].

#### 1. Quantum fluctuations in position and momentum

The action of the quantum measurement at the position  $j$  relates the postmeasurement state  $j^{(j)} i$  to the

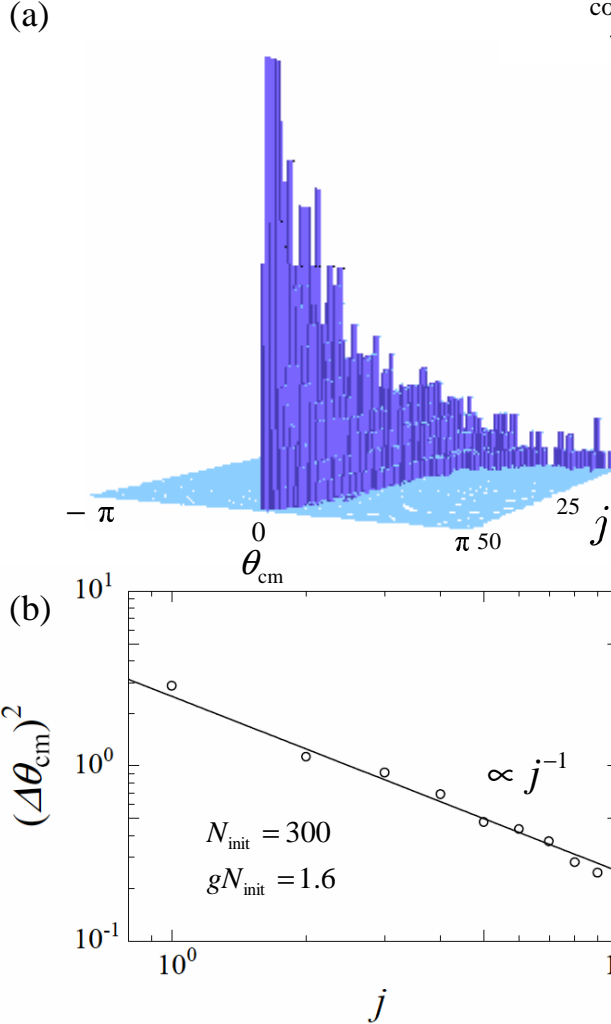


FIG. 10: (Color online) (a) Cumulative number of counts for the center-of-mass position obtained from 2000 runs of independent simulation of quantum measurements for  $gN_{\text{init}} = 1.6$  and  $N_{\text{init}} = 300$ . (b) Center-of-mass fluctuations obtained by the numerical simulations (open circles). The solid straight line obeys  $(\Delta\theta_{\text{cm}})^2 \propto j^{-1}$  and is drawn as a guide to the eye.

pre measurement state  $j^{(j-1)}i$  as

$$j^{(j)}i = \frac{\hat{y}^{(j)}j^{(j-1)}i}{h^{(j-1)}j\hat{y}^{(j)}\hat{y}^{(j)}j^{(j-1)}i}; \quad (21)$$

where  $j$  is the number of measurements, and the initial state  $j^{(j=0)}i$  is taken to be the many-body ground state. The subsequent measurement position  $j^{(j+1)}$  after the  $j$ th measurement is probabilistically determined according to the density distribution  $n_j(\cdot) = N_j^{(j)}(\cdot)$  of the pre-measurement state, where  $N_j = N_{\text{init}} - j$  is the number of atoms.

We perform 2000 runs of the numerical simulation of 50 quantum measurements (21) ( $0 \leq j \leq 50$ ) starting from the ground state with  $N_{\text{init}}$  atoms. By the measurements, the density distribution  $n_j(\cdot)$  is found to localize, and

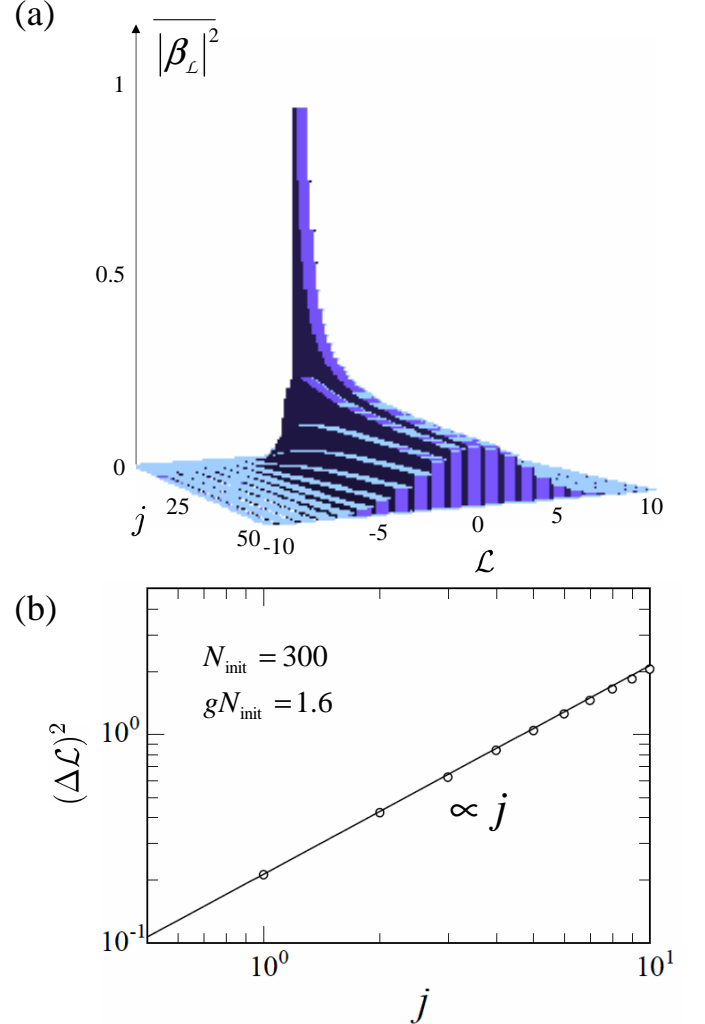


FIG. 11: (Color online) (a) Ensemble average of the angular momentum distribution  $j_L f$  obtained from 2000 runs of the numerical simulation, and (b) its width (open circles) for  $gN_{\text{init}} = 1.6$  and  $N_{\text{init}} = 300$ . The solid line is given by Eq. (65).

we denote the center-of-mass position of  $n_j(\cdot)$  by  $\hat{y}^{(j)}_{\text{cm}}$ . We find that as  $j$  increases,  $\hat{y}^{(j)}_{\text{cm}}$  converges to a certain position, which is random from run to run. We therefore rotate the system so that  $\hat{y}^{(j=50)}_{\text{cm}}$  is located at the origin, and plot the distribution of  $\hat{y}^{(j)}_{\text{cm}}$  for 2000 runs of measurements in Fig. 10(a). Hence, this distribution represents the center-of-mass fluctuation after the  $j$ th measurement. The variance of the distribution is plotted in Fig. 10(b), which shows that

$$(\Delta\theta_{\text{cm}})^2 \propto 1/j; \quad (22)$$

Because of the translation symmetry of the initial state  $j^{(j=0)}i$ , the center-of-mass fluctuation is maximal before the measurement. The repeated measurement process reduces the position fluctuation, and eventually projects the translation-invariant state  $j^{(j=0)}i$  onto a broken-

symmetry state whose center-of-mass localizes at a certain position.

Because the quantum measurement is a stochastic process, we consider the ensemble average of  $j_L \hat{j} = j_L j^{(j)} i \hat{j}$  over the 2000 runs of independent simulations. The result is shown in Fig. 11(a). We find from Fig. 11(b) that the distribution of the ensemble-averaged angular momentum obeys the Gaussian with its width given by

$$(L)^2 / j: \quad (23)$$

In the present 1D system, the center-of-mass position  $P_{cm}^N = \sum_{k=1}^N k = N$  and the angular momentum  $L = \sum_{k=1}^N (i\theta_k) = (\theta_k)$  obey the commutation relation

$$[cm, L] = i: \quad (24)$$

Their fluctuations  $cm: cm: h_{cm}: i$  and  $L: hL: i$  therefore obey

$$cm: L: \frac{1}{2}: \quad (25)$$

From Figs. 10 and 11, we found the uncertainty

$$cm: L: 0.73; \quad (26)$$

which is larger than that of the minimum uncertainty state.

## 2. Condensate fraction

We study the change in the condensate fraction as a function of the number of measurements  $j$ . In Fig. 12, we show the ensemble-averaged depleted fraction of the condensate in the state  $j^{(j)} i$  for three different values of the initial number of atoms  $N_{init}$ . The depletion decreases monotonically with increasing  $j$ . The change in the condensate fraction with respect to the number of measurements  $j$  is not sensitive to the initial number of atoms  $N_{init}$ , and is determined by  $gN_{init}$ . Like a symmetry-breaking potential, the repeated quantum measurements change the fragmented condensate having a translation symmetry into a translation-symmetry broken single condensate with reduced center-of-mass fluctuations.

## IV. BOGOLIUBOV AND EXTENDED MEAN-FIELD THEORIES

In the previous sections we showed that center-of-mass fluctuations are significant when the symmetry-breaking perturbations are sufficiently small. We here analytically treat the many-body state with large center-of-mass fluctuations for both cases of the symmetry-breaking potential and the quantum measurement.

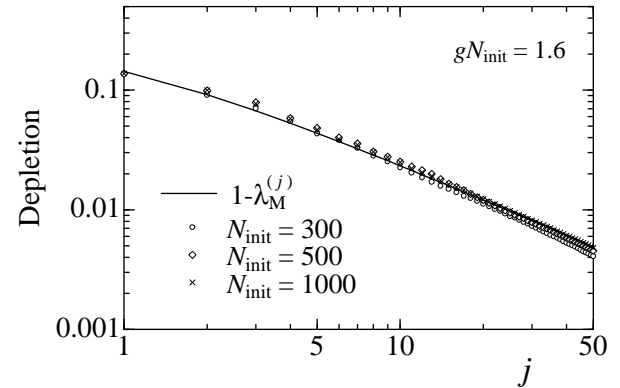


FIG. 12: Depletion of the condensate for  $gN_{init} = 1.6$ . Symbols ( ; , ) show the results of numerical simulations, and the solid curve shows a theoretical one in Eq. (69), where  $j$  is the number of measurements.

### A. Mean-field ground state in a homogeneous ring

By replacing the field operator with a complex number wave function as  $\psi(r) = (r)$ , we obtain GP energy functional

$$E_0^{(GP)}[r] = N \int_0^{Z_2} dr (r^2 + gN r^4): \quad (27)$$

We employ a variational wave function

$$\psi(r) = \frac{1}{\sqrt{2}} (r_0 + r_1 e^{i\phi} + r_1 e^{-i\phi}); \quad (28)$$

where  $r_0, r_1$  are complex variational parameters which obey the normalization condition  $r_0^2 + r_1^2 + r_1^2 = 1$  and are to be determined so as to minimize  $E_0^{(GP)}$ . For  $gN < 1$ ,  $E_0^{(GP)}$  is minimized when  $r_0 = 1; r_1 = 0$ , i.e., the condensate wave function is uniform,  $\psi(r) = 1/\sqrt{2}$ .

For  $gN = 1$ ,  $E_0^{(GP)}$  is minimized when

$$r_0 = \frac{\sqrt{3gN + 2}}{7gN}; \quad r_1 = r_1 = e^{i\phi} = \sqrt{\frac{2(gN - 1)}{7gN}}; \quad (29)$$

where the global phase is chosen so that  $r_0$  is real without loss of generality. The corresponding wave function

$$\psi(r) = \frac{1}{\sqrt{2}} [r_0 + \sqrt{2} r_1 \cos(\phi)]; \quad (30)$$

is a spontaneously broken-symmetry state. Note that all states described by Eq. (30) are degenerate with respect to an arbitrary center-of-mass coordinate  $\phi$ . The critical point  $gN = 1$  of the quantum phase transition obtained by the present mean-field theory agrees with the exact analysis of the 1D GP equation, and Eq. (29) indeed corresponds to the dominant coefficients of the plane-wave expansion of the exact solution of the 1D GP



where the parameter  $r$  is related to the Bogoliubov quasi-particle and hole amplitudes  $u$  and  $v$  by  $(\cosh r; \sinh r) / (u; v)$ . We evaluate the angular-momentum distribution in the Bogoliubov ground state

$$\begin{aligned} j^{(B)} i &= e^{\frac{r}{2}(\hat{T}^y)^2 - \frac{r^2}{2}} j_{\text{cm} := 0}^{(GP)} i \\ &= e^{\frac{r}{2}(\hat{T}^y)^2 - \frac{r^2}{2}} \frac{1}{N!} ({}_0 \hat{S}_0^y + \frac{p}{2} {}_1 \hat{S}_1^y)^N j_{\text{cm} := 0} i; \end{aligned} \quad (47)$$

where

$$\hat{S} = \frac{1}{2} (c_1 + c_1^*); \quad (48)$$

Let us approximate the angular-momentum operator

$$\hat{L} = \hat{n}_1 - \hat{n}_1 = \hat{S}^y \hat{T} + \hat{S} \hat{T}^y; \quad (49)$$

as

$$\hat{L}^2 = \hat{n}_1^2 = \frac{p}{2N} {}_1 (\hat{T} + \hat{T}^y); \quad (50)$$

by the replacement of  $\hat{S}$  with its mean-field value  $\frac{p}{2N} {}_1$  under the assumption that the ratio of the condensate atom  $s$  to the excited atom  $s$  is sufficiently large. By using the relation (see Appendix A for proof)

$$e^{\frac{r}{2}(\hat{T}^y)^2 - \frac{r^2}{2}} j_{\text{cm} := 0} i = \frac{1 + \frac{r}{\cosh r}}{\cosh r} e^{-\frac{r}{2}(\hat{T} + \hat{T}^y)^2} j_{\text{cm} := 0} i; \quad (51)$$

we obtain the Bogoliubov ground state as

$$j^{(B)} i = N_B \exp \left( -\frac{\hat{L}^2}{4N} \right) j_{\text{cm} := 0}^{(GP)} i; \quad (52)$$

where  $N_B$  is the normalization constant, and

$$\begin{aligned} &= \frac{\tanh r}{1 - \tanh r} = \frac{v=u}{1 - v=u} \\ &= \frac{r}{\frac{5gN + 2}{14}} = \frac{2gN}{3gN + 4} = \frac{1}{2} + O(\frac{1}{2}); \end{aligned} \quad (53)$$

We thus find that the angular-momentum distribution in the Bogoliubov ground state is given by

$$j_L j^{(B)} i = \frac{1}{2(L^{(B)})^2} e^{-\frac{L^2}{2(L^{(B)})^2}}; \quad (54)$$

where the width of this distribution is calculated to be (see Appendix B)

$$\begin{aligned} (L^{(B)})^2 &= N_1^2 = \\ &= \frac{2gN}{7gN} = \frac{2}{7} + O(\frac{1}{2}); \end{aligned} \quad (55)$$

with

$$F = \frac{7}{5gN + 2} = \frac{3gN + 4}{2gN + 2}; \quad (56)$$

The distribution of the angular momentum in  $j^{(B)} i$  is in excellent agreement with the distribution coefficient  $j_L j^{(B)} i$  in the many-body ground state (10) which is obtained numerically by the diagonalization of the Hamiltonian  $\hat{K}$  in Eq. (9).

### 3. Condensate fraction

The condensate fraction of the Bogoliubov ground state is less than unity because of virtual particle-pair excitations mainly to the translation mode. The virtual excitations are the physical origin of quantum fluctuations in the position and momentum described above. The number of depleted atoms is calculated from Eq. (39) as

$$N_B^0 = \frac{Z^2}{0} v^2(\text{cm}) d = \frac{1}{8} - \frac{1}{2} + O(\frac{p}{s}); \quad (57)$$

where  $v$  is given in Eq. (41). The result is shown as the solid line in Fig. 7 which agrees well with the results of the exact diagonalization for  $s_1$  &  $s_1$ .

We thus find that in the presence of the symmetry-breaking potential, the Bogoliubov ground state very well reproduces the energy, the angular-momentum distribution, and the depletion of the condensate obtained by the exact diagonalization for  $s_1$  &  $s_1$ . This is because the virtual excitations described by the Bogoliubov ground state lead to the center-of-mass fluctuations above the mean-field ground state.

### C. Quantum measurement

#### 1. Quantum fluctuations in position and momentum

In this section the suppression of the center-of-mass fluctuation via repeated quantum measurements shown in Fig. 10 is investigated semiclassically by generalizing mean-field theory. We assume as an initial state superposition state of the GP solution  $j_{\text{cm} := 0}^{(GP)} i$  with respect to the center-of-mass position  $\text{cm} := 0$ :

$$j_{\text{cm} := 0}^{(j)} i = d_{\text{cm} := 0} A_j(\text{cm} := 0) j_{\text{cm} := 0}^{(GP)} i; \quad (58)$$

We assume that for  $j = 0$ ,  $A_0(\text{cm} := 0)$  is a constant. The repeated measurements would select a localized soliton at a certain  $\text{cm} := 0$ ,  $A_j(\text{cm} := 0) = [{}_0 + 2 {}_1 \cos(\text{cm} := 0)] = \frac{1}{2}$  with probability  $A_j^2(\text{cm} := 0)$ . If the first atom is detected at a position  $\text{cm} := 1$ , the post-measurement distribution may be approximated by

$$A_1(\text{cm} := 1) = \frac{1}{2} [{}_0 + 2 {}_1 \cos(\text{cm} := 1)]; \quad (59)$$

where  ${}_0$  and  ${}_1$  are given by Eqs. (29). Likewise, after the  $j$ th measurement, the distribution becomes

$$A_j(\text{cm} := j) / \prod_{i=0}^{j-1} \frac{1}{2} [{}_0 + 2 {}_1 \cos(\text{cm} := i)]; \quad (60)$$

If we rotate the system so that  $\text{cm} := 0$  for  $j \neq 1$  (corresponding to the case of Fig. 10), the distribution of

$i$  should become  $[_0 + 2\_1 \cos \frac{\pi}{2}] = (2)$ . Equation (60) is then simplified for  $j = 1$  as

$$\ln A_j (cm) = \frac{X^j}{Z} \ln [1 + 2 \sum_{i=0}^1 \cos(i \pi cm)] + \text{const}$$

$$' j \quad d \ln ( ) \ln [1 + 2 \sum_{i=0}^1 \cos(i \pi cm)] + \text{const}$$

$$' 2j \sum_{i=1}^2 \frac{2}{cm} + \text{const} + \quad :$$

The distribution function of the center-of-mass position  $x_{cm}$  can thus be approximated as

$$A_j(c_m) / e^{-2j\frac{2}{1}c_m} = \dots \quad (62)$$

It follows then that the center-of-mass position fluctuates according to

$$cm : / \frac{1}{p_j} : \quad (63)$$

The angular momentum distribution of the state (58), can also be analytically calculated. Substituting Eq. (62) in Eq. (58), we find that the angular momentum distribution function is given by

$$\frac{1}{2 \cdot (L)^2} e^{-\frac{L^2}{2(L)^2}}; \quad (64)$$

with the width

$$(L)^2 = 2 \begin{smallmatrix} 2 \\ 1 \end{smallmatrix} j: \quad (65)$$

It follows from Eqs. (63) and (65) that during the repeated measurements the fluctuations in the center of mass and the angular momentum are found to obey the uncertainty relation

$$cm : L' 1 : \quad (66)$$

Both Eqs. (63) and (65) are in excellent agreement with the ensemble averages of the corresponding results obtained by the numerical simulation as shown in Figs. 10 and 11.

## 2. Condensate fraction

We showed in the previous section that the repeated measurements suppress the center-of-mass fluctuations. We show here that this leads to an enhancement of the condensate fraction. The reduced single-particle density matrix of  $j$  is obtained from Eqs. (44), (58), and (62) as

$$(1; \overset{0}{1}) = \frac{hc^y}{2} \overset{1}{e}_1 \overset{1}{e}_1$$

$$! \quad 4 \quad \overset{2}{0} \quad \overset{1}{1} \overset{1}{e} = 2 \quad \overset{0}{1} \overset{2}{e} = 2 \quad \overset{2}{1} \overset{2}{e} = 3$$

$$\overset{2}{1} \overset{2}{e} \quad \overset{0}{1} \overset{1}{e} = 2 \quad \overset{2}{1} \overset{2}{e} = 5; \quad (67)$$

where  $1 = (8 \begin{smallmatrix} 2 \\ 1 \end{smallmatrix} j)$ , and we assumed

for simplicity. The largest eigenvalue  $\lambda_M^{(j)}$  of  $(I; f)$  is given by

$$(61) \quad \frac{M^{(j)}}{Q} = \frac{1}{2} \cdot 1 + \frac{2}{1} e^2 + \frac{4}{1} \cdot \frac{2}{1} (1 + \frac{2}{1} e^2)^2 \quad : (69)$$

Figure 12 compares Eq. (69) with the results obtained by numerical diagonalization, where the quantitative agreement is found. Like a symmetry-breaking potential, the repeated quantum measurements also change the fragmented condensate with a translation symmetry to a single condensate with a broken translation symmetry. In terms of the generalized mean-field theory developed in this section, the depletion of atoms is described by the amplitude  $A_j$  in the state (58), the absolute square of which represents the semiclassical distribution function of the center of mass of the bright soliton.

## V. SUMMARY AND CONCLUSIONS

We have investigated the critical fluctuations associated with the formation of broken-symmetry state by explicitly introducing symmetry-breaking potentials or quantum measurements.

In the absence of the symmetry-breaking potential, the many-body ground state, obtained by the diagonalization of the symmetry-preserving Hamiltonian, is found to be fragile against a formation of a localized state. The localized state corresponds to a superposition state of quasidegenerate low-lying modes. The localization is also reflected in the enhancement in the two-body correlation.

In Sec. IIIA, we have studied the many-body localized state in the presence of an infinitesimal symmetry-breaking potential. We have shown that the localization of the many-body ground state begins when the energy scale of the symmetry-breaking potential becomes of the same order of the energy gap between the ground and the first excited state of the symmetry-preserving Hamiltonian, i.e.,  $1 \approx N$ . We have evaluated center-of-mass fluctuations in the regime of the crossover between the state with the translation symmetry and the broken-symmetry state, and found that these fluctuations are the origin of the depletion of the condensate fraction. In the presence of the double-well potential, we have shown that as the magnitude of the potential is increased, the ground state becomes a Schrödinger's cat state, i.e., the macroscopic superposition of two localized states.

In a manner similar to the single-potential case, repeated quantum measurements also cause the crossover from the uniform state to the localized state with significant enhancement in the condensate fraction. We

have shown that the center-of-mass and the angular-momentum fluctuations obey the uncertainty relation (26) during quantum measurements.

In the latter part of this paper, we have developed an analytic method to treat the many-body states with quantum fluctuations. Starting from the broken-symmetry ground state of the GP equation, we have taken into account the translation mode of the soliton as a Bogoliubov fluctuation in the presence of an inhomogeneous symmetry-breaking potential. We have found that the angular-momentum fluctuations and the condensate fraction of the Bogoliubov ground state very well agrees with those of the numerically obtained many-body localized state.

The effects of the quantum measurement of the bright soliton on the localization have been studied by developing a generalized mean-field theory, where we introduce a semiclassical distribution function of the center-of-mass position of the soliton. Assuming as an initial state an isotropic superposition of soliton states, we have argued that the measurement process reduces the center-of-mass fluctuation and selects a soliton state having a definite center of mass. The results obtained by the extended mean-field theory and those obtained by the numerical simulation using the symmetry-preserving Hamiltonian agree excellently in terms of the angular-momentum fluctuation, the center-of-mass fluctuation, and the condensate fraction.

We have thus shown that the critical fluctuations associated with the formation of a localized BEC with an attractive interaction arise from quantum fluctuations in the position of the matter wave, which is also interpreted as the depletion of the condensate to the translation modes of the bright soliton.

## VI. ACKNOWLEDGEMENTS

This work was supported by Grants-in-Aids for Scientific Research (Grant No. 15340129, No. 17071005, and No. 17740263) and by a 21st Century COE program at Tokyo Tech "Nanometer-Scale Quantum Physics," from the Ministry of Education, Culture, Sports, Science and Technology of Japan. M. J. acknowledges support by a CREST program of the JST.

## APPENDIX A: DERIVATION OF OPERATOR RELATION (51)

In order to prove the relation (51), we disentangle two operators

$$\hat{O}_1 = e^{\frac{r}{2}(\hat{T}^y)^2 - \hat{T}^2}; \quad (A 1)$$

$$\hat{O}_2 = e^{\frac{r}{2}(\hat{T}^y + \hat{T})^2}; \quad (A 2)$$

We define an unnormalized state

$$|j\rangle = e^{\hat{T}^y} |j\rangle_{\text{aci}}; \quad (A 3)$$

where  $j$  is a complex number, and define the expectation value of  $\hat{O}_j$  ( $j = 1, 2$ ) with respect to the state  $|j\rangle$  as

$$\langle j | \hat{O}_j | j \rangle_{\text{aci}}; \quad (A 4)$$

The derivatives of  $\langle j | \hat{O}_j | j \rangle$  with respect to  $r$  and  $\theta$  are given by

$$\frac{\partial \langle j | \hat{O}_j | j \rangle}{\partial r} = h \hat{O}_j \hat{T}^y | j \rangle_{\text{aci}} = h \hat{O}_j \hat{T}^y \hat{O}_j^{-1} \hat{O}_j | j \rangle_{\text{aci}}; \quad (A 5)$$

$$\frac{\partial \langle j | \hat{O}_j | j \rangle}{\partial \theta} = h \hat{T}^y \hat{O}_j | j \rangle_{\text{aci}} = h \hat{O}_j \hat{O}_j^{-1} \hat{T}^y \hat{O}_j | j \rangle_{\text{aci}}; \quad (A 6)$$

By using the relations

$$\hat{O}_1^{-1} \hat{T} \hat{O}_1 = \hat{T} \cosh r - \hat{T}^y \sinh r; \quad (A 7)$$

$$\hat{O}_1 \hat{T}^y \hat{O}_1^{-1} = \hat{T}^y \cosh r + \hat{T} \sinh r; \quad (A 8)$$

$$\hat{O}_2^{-1} \hat{T} \hat{O}_2 = \hat{T} - (\hat{T} + \hat{T}^y); \quad (A 9)$$

$$\hat{O}_2 \hat{T}^y \hat{O}_2^{-1} = \hat{T}^y - (\hat{T} + \hat{T}^y); \quad (A 10)$$

we obtain

$$\frac{\partial \langle j | \hat{O}_1 | j \rangle}{\partial r} = \cosh r \langle j | \hat{O}_1 | j \rangle + \sinh r \frac{\partial \langle j | \hat{O}_1 | j \rangle}{\partial \theta}; \quad (A 11)$$

$$\frac{\partial \langle j | \hat{O}_1 | j \rangle}{\partial \theta} = \cosh r \langle j | \hat{O}_1 | j \rangle - \sinh r \frac{\partial \langle j | \hat{O}_1 | j \rangle}{\partial r}; \quad (A 12)$$

$$\frac{\partial \langle j | \hat{O}_2 | j \rangle}{\partial r} = (1 - \langle j | \hat{O}_2 | j \rangle) \frac{\partial \langle j | \hat{O}_2 | j \rangle}{\partial \theta}; \quad (A 13)$$

$$\frac{\partial \langle j | \hat{O}_2 | j \rangle}{\partial \theta} = (1 - \langle j | \hat{O}_2 | j \rangle) \frac{\partial \langle j | \hat{O}_2 | j \rangle}{\partial r}; \quad (A 14)$$

The differential equations for  $\langle j | \hat{O}_j | j \rangle$  are then given by

$$\frac{\partial \langle j | \hat{O}_1 | j \rangle}{\partial r} = \frac{1 + \sinh r}{\cosh r} \langle j | \hat{O}_1 | j \rangle; \quad (A 15)$$

$$\frac{\partial \langle j | \hat{O}_1 | j \rangle}{\partial \theta} = \frac{\sinh r}{\cosh r} \langle j | \hat{O}_1 | j \rangle; \quad (A 16)$$

$$\frac{\partial \langle j | \hat{O}_2 | j \rangle}{\partial r} = \frac{1}{1 + \sinh r} (1 - \langle j | \hat{O}_2 | j \rangle) \langle j | \hat{O}_2 | j \rangle; \quad (A 17)$$

$$\frac{\partial \langle j | \hat{O}_2 | j \rangle}{\partial \theta} = \frac{1}{1 + \sinh r} (1 - \langle j | \hat{O}_2 | j \rangle) \langle j | \hat{O}_2 | j \rangle; \quad (A 18)$$

By integrations of these equations, the expectation values  $\langle j | \hat{O}_1 | j \rangle$  and  $\langle j | \hat{O}_2 | j \rangle$  are found to be

$$\langle j | \hat{O}_1 | j \rangle = e^{\frac{1}{2} \tanh r - 2 + \frac{1}{\cosh r} j^2 - \frac{1}{2} \tanh r^2}; \quad (A 19)$$

$$\langle j | \hat{O}_2 | j \rangle = e^{\frac{1}{2} \frac{1}{1 + \sinh r} - 2 + \frac{1}{1 + \sinh r} j^2 - \frac{1}{2} \frac{1}{1 + \sinh r}^2}; \quad (A 20)$$

The operators  $\hat{O}_j$  are thus written as

$$\hat{O}_1 = e^{\frac{r}{2}(\hat{T}^y)^2} e^{\ln(\cosh r) \hat{T}^y \hat{T}} e^{\frac{1}{2} \tanh r \hat{T}^2}; \quad (A 21)$$

$$\hat{O}_2 = e^{\frac{r}{2}(1 + \sinh r) \hat{T}^y \hat{T}} e^{\ln(1 + \sinh r) \hat{T}^y \hat{T}} e^{\frac{1}{2} (1 + \sinh r) \hat{T}^2}; \quad (A 22)$$

and we finally obtain

$$e^{\frac{r}{2}(\hat{T}^y)^2} |j\rangle_{\text{aci}} = N_1 e^{\frac{1}{2} \hat{T}^y \tanh r} |j\rangle_{\text{aci}}; \quad (A 23)$$

$$e^{\frac{r}{2}(\hat{T}^y + \hat{T})^2} |j\rangle_{\text{aci}} = N_2 e^{\frac{1}{2} \hat{T}^y \tanh r} |j\rangle_{\text{aci}}; \quad (A 24)$$

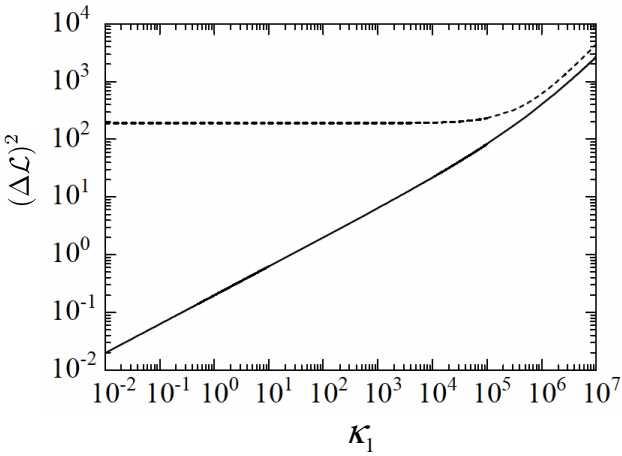


FIG. 13: Width of the angular momentum fluctuations in the GP ground state  $j^{(GP)}i$  (dashed curve) and that in the state  $e^{\frac{r}{2}(\hat{f}^{y2} - \hat{f}^2)}j_{\text{aci}}$  (solid curve).

where the normalization constants  $N_j$  are determined by

$$1 = \hbar v a c \hat{D}_1^{-1} \hat{O}_1 j_{\text{aci}} = N_1^2 \sum_n \frac{2n!}{(n!)^2} \frac{1}{2} \tanh r^{2n} = N_1^2 \cosh r; \quad (\text{A } 25)$$

$$1 = \hbar v a c \hat{D}_2^{-1} \hat{O}_2 j_{\text{aci}} = N_2^2 \sum_n \frac{2n!}{(n!)^2} \frac{1}{2(1+)^{2n}} = N_2^2 (1+); \quad (\text{A } 26)$$

#### APPENDIX B : EVALUATION OF ANGULAR-MOMENTUM FLUCTUATION IN THE BOGOLIUBOV GROUND STATE

We justify the approximation, Eq. (54) with Eq. (55), that has been used in order to evaluate the angular-

momentum fluctuation  $(L^{(B)})^2$  in the Bogoliubov ground state

$$j^{(B)}i = e^{\frac{r}{2}(\hat{f}^{y2} - \hat{f}^2)} \frac{1}{p!} \left( \frac{1}{N!} (j_0^{(Y)} + \frac{p}{2} j_1^{(Y)})^N \right) j_{\text{aci}}; \quad (\text{B } 1)$$

The angular-momentum distribution of the GP ground state  $j^{(GP)}i = \frac{1}{N!} (j_0^{(Y)} + \frac{p}{2} j_1^{(Y)})^N j_{\text{aci}}$  is calculated to give

$$j^{(L)} j^{(GP)} = j_0^{(Y)} / \sum_{n=1}^{N-2} \frac{1}{(N-L-2n)!(L+n)!n!} \frac{j_1^{(Y)}}{j_0^{(Y)}}^{4n} \cdot \frac{1}{p!} \frac{1}{2(L^{(GP)})^2} e^{-\frac{L^2}{2(L^{(GP)})^2}}; \quad (\text{B } 2)$$

where  $j_0$  and  $j_1$  are given in Eqs. (33) and (34), and the width is given by

$$(L^{(GP)})^2 = \frac{2N}{2 + j_0^2/j_1^2}; \quad (\text{B } 3)$$

On the other hand, from the form of Eq. (52), the angular-momentum fluctuation operator  $e^{\frac{r}{2}(\hat{f}^{y2} - \hat{f}^2)}$  approximately gives the factor

$$\exp \frac{L^2}{2(L^{(B)})^2} \quad (\text{B } 4)$$

to the state with an angular momentum  $L$ , where the width  $(L^{(B)})$  is given in Eq. (55). The angular-momentum distribution of  $j^{(B)}i$  is given by the product of Eqs. (B2) and (B4). We compare Eqs. (B3) and (55) in Fig. 13, where the former is much larger than the latter for  $L \gtrsim 10^4$ . Therefore, the contribution from Eq. (B2) is negligible, and the angular-momentum distribution of  $j^{(B)}i$  can be approximated by Eq. (B4).

---

[1] S. Richard, F. Gerbier, J.H. Thywissen, M. Hugbart, P. Bouyer, and A. Aspect, *Phys. Rev. Lett.* **91**, 010405 (2003).  
[2] D. Hellweg, L. Cacciapuoti, M. Kottke, T. Schulte, K. Sengstock, W. Ertmer, and J.J. Arlt, *Phys. Rev. Lett.* **91**, 010406 (2003).  
[3] C. Orzel, A.K. Tuchman, M.L. Fenselau, M. Yamada, and M.A.K. Kasevich, *Science* **291**, 2386 (2001).  
[4] E.M. Wright, D.F. Walls, and J.C. Garrison, *Phys. Rev. Lett.* **77**, 2158 (1996).  
[5] M. Lewenstein and L. You, *Phys. Rev. Lett.* **77**, 3489 (1996).  
[6] C.K. Law, H. Pu, and N.P. Bigelow, *Phys. Rev. Lett.* **81**, 5257 (1998).  
[7] M. Kashi and M. Ueda, *Phys. Rev. Lett.* **84**, 1066 (2000).  
[8] T.-L. Ho and S.-K. Yip, *Phys. Rev. Lett.* **84**, 4031 (2000).  
[9] S.Y. Yi, O.E. Moustecaplioglu, and L. You, *Phys. Rev. Lett.* **90**, 140404 (2005).  
[10] M.H.W. Beeler, K.M. Mertes, J.D. Erwin, and D.S. Hall, *Phys. Rev. Lett.* **93**, 170402 (2004).  
[11] S. Ashhab and A.J. Leggett, *Phys. Rev. A* **68**, 063612 (2003).  
[12] N.R. Cooper, N.K.W. Wilkin, and J.M.F. Gunn, *Phys. Rev. Lett.* **87**, 120405 (2001).  
[13] T.Nakajima and M. Ueda, *Phys. Rev. A* **63**, 043610 (2000).  
[14] R.Kanamoto, H. Saito, and M. Ueda, *Phys. Rev. Lett.* **94**, 090404 (2005).  
[15] V.E. Zakharov and A.B. Shabat, *Zh. Eksp. Teor. Fiz.* **61**, 118 (1971) [Sov. Phys. JETP **34**, 62 (1972)].  
[16] Y. Castin and C. Herzog, e-print cond-mat/0012040, *Comptes Rendus de l'Academie des Sciences de Paris, tome 2, serie IV*, p.419-443 (2001)].

[17] O.E. Alon, A.I. Streltsov, and L.S. Cederbaum, *Phys. Rev. B* 71, 125113 (2005).

[18] S. Gupta, K.W. Murch, K.L. Moore, T.P. Purdy, and D.M. Stamps-Kum, *Phys. Rev. Lett.* 95, 143201 (2005).

[19] O. Penrose and L. Onsager, *Phys. Rev.* 104, 576 (1956).

[20] P. Nozieres and D. Saint James, *J. Phys. (France)* 43, 1133 (1982).

[21] R. Kanamoto, H. Saito, and M. Ueda, *Phys. Rev. A* 67, 013608 (2003).

[22] When the system is subjected to a rotating drive, the degeneracy with respect to  $E_L$  is lifted. For a strong coupling regime the angular momentum  $L_g$  in the ground state can increase. The superposition for the localized state in this case is given by  $j^{(1)}i = e^{i\int_0^P \mathcal{J}_g dt} + \sum_{L>0} \frac{1}{L} (j_g + L i + j_g - L i)$  instead of Eq. (10). The angular momentum thus fluctuates around  $L_g$ , and the center of mass also fluctuates with the width  $\propto 1/(L)^{1/2}$ .

[23] Y. Shin, M. Saba, T.A. Pasquini, W. Ketterle, D.E. Pritchard, and A.E. Leanhardt, *Phys. Rev. Lett.* 92, 050405 (2004).

[24] T.-L. Ho and C.V. Ciobanu, *J. Low. Temp. Phys.* 135, 257 (2004).

[25] J.I. Cirac, M. Lewenstein, K. M. M[ü]ller, and P. Zoller, *Phys. Rev. A* 57, 1208 (1998).

[26] M.J. Steel and M.J. Collett, *Phys. Rev. A* 57, 2920 (1998).

[27] M.W. Jack and M. Yamashita, *Phys. Rev. A* 71, 023610 (2005).

[28] J. Javanainen and S.M. Yoo, *Phys. Rev. Lett.* 76, 161 (1996).

[29] Y. Castin and J. Dalibard, *Phys. Rev. A* 55, 4330 (1997).

[30] A. Montina and F.T. Arcelli, *Phys. Rev. A* 71, 063615 (2005).

[31] L.D. Carr, C.W. Clark, and W.P. Reinhardt, *Phys. Rev. A* 62, 063611 (2000).